Antimalarial N1,N3-dialkyldioxonaphthoimidazoliums: Synthesis, biological activity and structure-activity relationships.

Stephen Ahenkorah, ^ ‡ Dina Coertzen, ϕ‡ Jie Xin Tong, # ‡ Kevin T. Fridianto, §‡ Sergio Wittlin, √¥ Lyn-Marie Birkholtz, ϕ Kevin Shyong Wei Tan, # Yulin Lam, § Mei Lin Go, ^ * Richard K. Haynes. ¶ *

^ Department of Pharmacy, # Department of Microbiology and Immunology and § Department of Chemistry, National University of Singapore, Singapore 117543; ϕ Institute for Sustainable Malaria Control, Department of Biochemistry, Genetics and Microbiology, University of Pretoria, South Africa 0028; √ Swiss Tropical and Public Health Institute, Switzerland 4051; ¥ University of Basel, Switzerland 4003, ¶ Centre of Excellence for Pharmaceutical Sciences, North-West University, South Africa 2531.

KEYWORDS   Antimalarials; Dioxonaphthoimidazoliums; Quinones; Drug resistant asexual parasites; Gametocytocidal activity.

Abstract: Here we report the nanomolar potencies of N^1, N^3-dialkyldioxonaphthoimidazoliums against asexual forms of sensitive and resistant *Plasmodium falciparum*. Activity was dependent on the presence of the fused quinone-imidazolium entity and lipophilicity imparted by the N^1/ N^3 alkyl residues on the scaffold. Gametocytocidal activity was also detected, with most members active at IC_{50} < 1 μM. A representative analog with good solubility, limited PAMPA permeability and microsomal stability, demonstrated oral efficacy on a humanized mouse model of *P. falciparum*.

Substantial progress has been made in decreasing the global burden of malaria over the past decade. Worldwide, 20 million fewer cases of malaria were recorded in 2017 as compared to 2010.[1] Deaths due to malaria have declined, from 607 000 in 2010 to 435 000 in 2017.[1] Furthermore, low attrition rates among recent clinical trial candidates hint at a potentially rich antimalarial drug pipeline in the offing.[2] However, optimism engendered by these encouraging statistics belie two worrying trends. First, several high burden countries on the African continent have seen a resurgence in malaria in spite of vigorous efforts to curtail spread.[1] Second, the Greater Mekong Region has witnessed intensification of the multidrug-resistant *Plasmodium falciparum* co-lineage KEL1/PLA1.[3] These events highlight the fragility of gains made against malaria and the need for constant vigilance if they are to be sustained. Like

other infectious diseases, the emergence of resistant parasite strains is a question of *when* and not *if*. Regardless of the prevailing optimism invoked by the current status of the drug pipeline, there is a constant need for new agents to protect vulnerable populations, prevent relapses of vivax infection and disrupt disease transmission.[2] Eradication of malaria which is a key Millennium Development Goal set by the United Nations, is achieved only by breaking disease transmission.[4] Unlike malaria control which treats the symptoms caused by asexual parasites, eradication focuses on eliminating the sexual forms (gametocytes) which are directly responsible for infecting the anopheline vector and perpetuating the plasmodial life cycle. Ideally, antimalarial leads should target both asexual and sexual intraerythrocytic parasites with comparable potencies.[5]
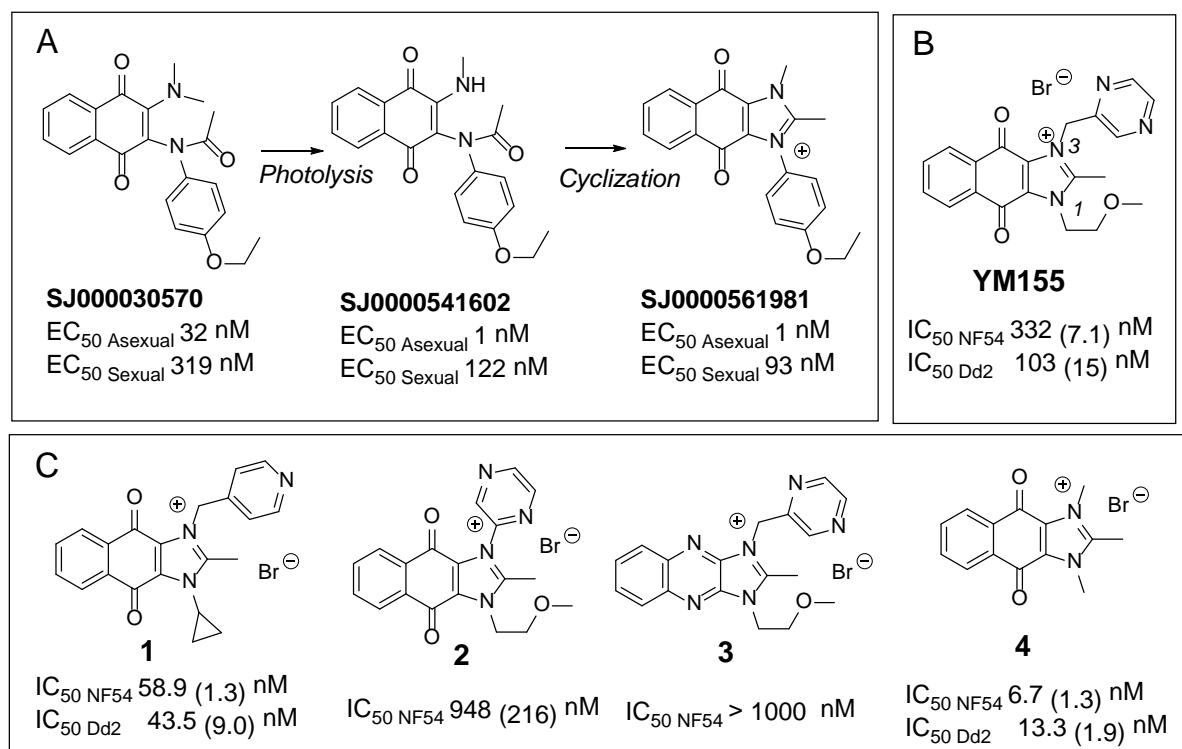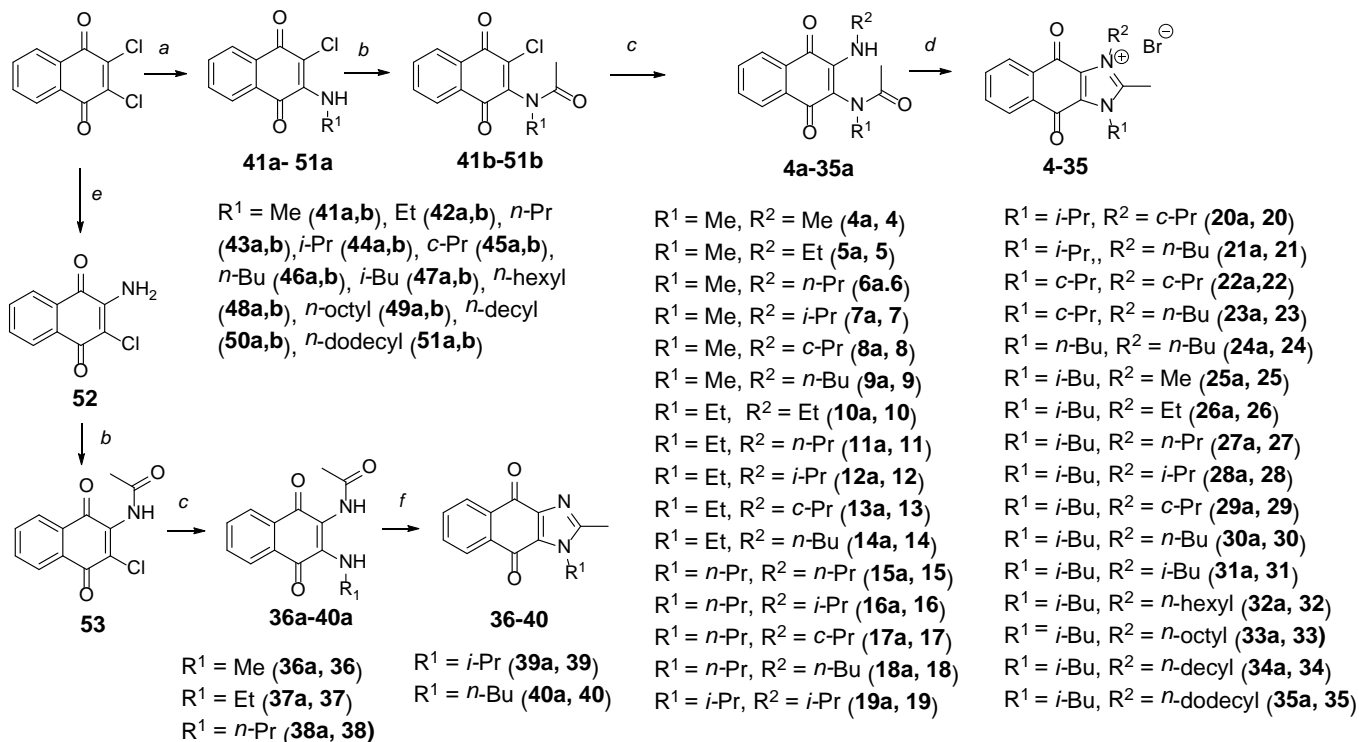

Figure 1: (A) Stepwise conversion of SJ000030570 to SJ0000541602 and SJ0000561981 and their EC_{50}s against the asexual and sexual stages of *P. falciparum* 3D7.[6] Structures of (B) YM155 (C) analogs **1-4** [7] and their IC_{50}s (± SD) against asexual stages of drug sensitive NF54 and drug resistant Dd2 *P. falciparum.* Parasitemia was assessed by the parasite lactate dehydrogenase assay. Positive controls were chloroquine ($IC_{50\ NF54}$ 8.2 ±0.4 nM; $IC_{50\ Dd2}$ 118 ±3 nM) and artesunate ($IC_{50\ NF54}$ < 5 nM; $IC_{50\ Dd2}$ 18.8 ±1.5 nM).

In an effort to identify lead compounds with potent activity against both life-cycle stages of *P. falciparum*, Tanaka and co-workers reported the demethylation of the diaminonaphthoquinone SJ000030570 to the monomethylamino analog SJ0000541602 on prolonged exposure to light, followed by cyclization of the latter to the dioxonaphthoimidazolium SJ0000561981 (Figure 1A).[6] Both SJ0000541602 and SJ0000561981 were photostable and exceptionally potent against asexual ring stages and late stage (Stage III-V) gametocytes (Figure 1A).[6]

The dioxonaphthoimidazolium scaffold of SJ0000561981 is present in YM155 (sepantronium bromide, Figure 1B), an antitumor agent and suppressor of the anti-apoptotic protein survivin.[8] This prompted us to ask if YM155 could emulate the antimalarial activity of SJ0000561981 and more importantly, if the scaffold is an incipient antimalarial pharmacophore. Hence, YM155 and several analogs (**1-4**) that were previously investigated on human cancer cell lines [7] were screened against the erythrocytic stages of drug sensitive and drug resistant *P. falciparum* (Figure 1B). Disappointingly, YM155 displayed only modest activity but its analogs **1** and 4 proved more potent. We were particularly intrigued by **4** whose outstanding activity is ostensibly linked to the absence of cyclized entities at the ring nitrogens N^1/N^3. This led us to propose modifying the alkyl substituents in **4** by homologation or branching as a means of optimizing the antimalarial potential of the scaffold. To this end, a series of N^1,N^3-dialkyldioxonaphthoimidazoliums (**4-35**) were synthesized and evaluated against the asexual and sexual intraerythrocytic stages of *P. falciparum*.

Briefly, our target compounds were obtained by introducing alkyl groups and their branched/cyclized variants at one of the imidazolium N atoms while retaining an unchanged alkyl at the other N atom. For instance, with methyl at N^1, we inserted ethyl, propyl, butyl, isopropyl or cyclopropyl in turn at N^3 and this was repeated with each of the aforementioned N^3 substituents at N^1. In this way, Series A (**4-24**) was prepared and evaluated on the asexual stages of *P. falciparum*. The results prompted the synthesis of two additional series, namely the non-quaternized Series B (**36-40**) in which only N^1 was substituted and Series C (**25-35**) which has isobutyl at N^1, the same groups at N^3 as in Series A in addition to longer alkyl side chains (isobutyl, n-hexyl, n-octyl, n-decyl, n-dodecyl) (Scheme 1). Several members in Series A-C have been reported in the literature, namely **4,10,19**; [9] **5,7,9,11,14,16,25,36-40**; [10] **24,31**; [11] **12,13**;[12] and **15**. [13] We followed the method of Ho *et al.*[7] to obtain Series A-C.

Scheme 1 [a]

41a- 51a **41b-51b** **4a-35a** **4-35**

R[1] = Me (**41a,b**), Et (**42a,b**), n-Pr
(**43a,b**), i-Pr (**44a,b**), c-Pr (**45a,b**),
n-Bu (**46a,b**), i-Bu (**47a,b**), n-hexyl
(**48a,b**), n-octyl (**49a,b**), n-decyl
(**50a,b**), n-dodecyl (**51a,b**)

R[1] = Me, R[2] = Me (**4a, 4**)
R[1] = Me, R[2] = Et (**5a, 5**)
R[1] = Me, R[2] = n-Pr (**6a.6**)
R[1] = Me, R[2] = i-Pr (**7a, 7**)
R[1] = Me, R[2] = c-Pr (**8a, 8**)
R[1] = Me, R[2] = n-Bu (**9a, 9**)
R[1] = Et, R[2] = Et (**10a, 10**)
R[1] = Et, R[2] = n-Pr (**11a, 11**)
R[1] = Et, R[2] = i-Pr (**12a, 12**)
R[1] = Et, R[2] = c-Pr (**13a, 13**)
R[1] = Et, R[2] = n-Bu (**14a, 14**)
R[1] = n-Pr, R[2] = n-Pr (**15a, 15**)
R[1] = n-Pr, R[2] = i-Pr (**16a, 16**)
R[1] = n-Pr, R[2] = c-Pr (**17a, 17**)
R[1] = n-Pr, R[2] = n-Bu (**18a, 18**)
R[1] = i-Pr, R[2] = i-Pr (**19a, 19**)

R[1] = i-Pr, R[2] = c-Pr (**20a, 20**)
R[1] = i-Pr,, R[2] = n-Bu (**21a, 21**)
R[1] = c-Pr, R[2] = c-Pr (**22a,22**)
R[1] = c-Pr, R[2] = n-Bu (**23a, 23**)
R[1] = n-Bu, R[2] = n-Bu (**24a, 24**)
R[1] = i-Bu, R[2] = Me (**25a, 25**)
R[1] = i-Bu, R[2] = Et (**26a, 26**)
R[1] = i-Bu, R[2] = n-Pr (**27a, 27**)
R[1] = i-Bu, R[2] = i-Pr (**28a, 28**)
R[1] = i-Bu, R[2] = c-Pr (**29a, 29**)
R[1] = i-Bu, R[2] = n-Bu (**30a, 30**)
R[1] = i-Bu, R[2] = i-Bu (**31a, 31**)
R[1] = i-Bu, R[2] = n-hexyl (**32a, 32**)
R[1] = i-Bu, R[2] = n-octyl (**33a, 33**)
R[1] = i-Bu, R[2] = n-decyl (**34a, 34**)
R[1] = i-Bu, R[2] = n-dodecyl (**35a, 35**)

52

53 **36a-40a** **36-40**

R[1] = Me (**36a, 36**)
R[1] = Et (**37a, 37**)
R[1] = n-Pr (**38a, 38**)

R[1] = i-Pr (**39a, 39**)
R[1] = n-Bu (**40a, 40**)

[a] Reagents and conditions (a) R[1]-amine, EtOH, r.t, 18h; (b) acetic anhydride, conc H_2SO_4, r.t,
1.5 h; (c) R[2]-amine, toluene, 45 °C, 4 h; (d) 48% HBr (aq), EtOH + EtOAc, 45 °C , 4h to r.t
overnight; (e) NH_3 in MeOH, EtOH, 35 °C, 3 h; (f) 48% HBr (aq), 2M NaOH (2 drops), EtOH,
50 °C, 1h.

The growth inhibitory IC_{50}s of Series A compounds on the asexual forms of Dd2 (drug
resistant) and 3D7 (drug sensitive) strains of *P. falciparum* were determined by a Hoechst
33342-based method with a fluorescence-activated cell sorter (FACS) to measure DNA
content of infected erythrocytes.[14] Encouragingly, all the compounds displayed sub-micromolar
activities on both Dd2 and 3d7 with broadly similar levels of potencies but with some
exceptions (**17, 23**) (Table 1). In addition, we found excellent differential cytotoxicities in this
series, with most compounds associated with a 100-fold or greater selectivity vis-à-vis
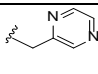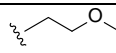mammalian Chinese hamster ovary (CHO) cells.

The most potent compounds were **11, 14, 16, 19** which had low nanomolar activities (IC_{50} < 10 nM) against both resistant and sensitive plasmodia. Interestingly, the total carbon count on R^1/R^2 of these compounds was either 5 or 6, out of a possible range of 2 to 8. Hence, we posited that optimal activity resided within a narrow spectrum, tentatively defined by 5-6 carbons, with declining potencies at either end of this range. Indeed, diminished activity was evident in the dibutyl analog **24** while short hydrophilic fragments like methyl and cyclopropyl were disproportionally represented at R^1/R^2 of less potent analogs such as **4, 5, 8** and **13**. The hydrophilicity of the cyclopropyl fragment, anomalous for its carbon count, is attributed to its unique three-dimensional features.[15]

Earlier, we observed significantly diminished antimalarial activity in the non-quinoid analog **3** of YM155 (Figure 1C) which portend a pivotal structure-activity role for the quinone. However, only modest activity was uncovered in representative quinones like 1,4-naphthoquinone, menadione and 1,4-benzoquinone against NF54 asexual parasites (20-40% inhibition at 1 µM, Table S-2). Hence, we posited that it was not the quinone per se but the fusion of the quinone to the charged imidazolium ring that was required for potent activity. Consequently, we synthesized Series B (**36-40**) in which the quinone is fused to an uncharged alkyl substituted imidazole ring (Scheme 1). Gratifyingly, no member in this series inhibited growth by more than 50% at 1 µM (Table S-2), thus affirming the essentiality of the fused quinone-imidazolium for potent activity.

Table 1: Growth inhibitory activities of Series A (**4-24**) on asexual ring stages of *P. falciparum* Dd2 (drug resistant), 3D7 (drug sensitive) and mammalian Chinese Hamster Ovary (CHO) cells.
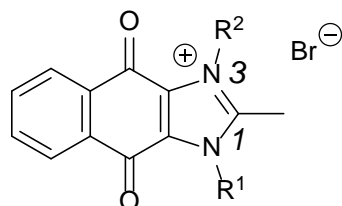
No	R^1 [a]	R^2 [a]	IC$_{50}$ expressed as Mean ± SD		
			Dd2 (nM)[b]	3D7 (nM)[b]	CHO (µM)[c]
4	CH_3	CH_3	26.5 ±2.6	22.6 ±1.1	5.7 ±1.1
5	CH_3	C_2H_5	19.9 ±0.3	8.4 ±4.7	3.6 ±2.1
6	CH_3	n-C_3H_7	14.3 ±0.6	4.8 ±2.6	3.9 ±0.6
7	CH_3	i-C_3H_7	16.1 ±1.1	4.8 ±2.3	4.7 ±2.3
8	CH_3	c-C_3H_7 [d]	30.4 ±6.3	25.7 ±3.3	3.1 ±0.9
9	CH_3	n-C_4H_9	14.1 ±0.8	4.3 ±1.5	13.1 ±1.1
10	C_2H_5	C_2H_5	19.1 ±2.8	6.0 ±0.7	14.7 ±1.0
11	C_2H_5	n-C_3H_7	8.4 ±2.1	3.7 ±0.5	8.2 ±0.3
12	C_2H_5	i-C_3H_7	11.7 ±1.3	61.5 ±12.7	15.1 ±1.6
13	C_2H_5	c-C_3H_7 [d]	35.0 ±5.5	66.1 ±19	6.6 ±0.5
14	C_2H_5	n-C_4H_9	9.1 ±4.2	4.2 ±0.2	37.0 ±1.2
15	n-C_3H_7	n-C_3H_7	11.3 ±3.4	26.9 ±20	16.2 ±0.5
16	n-C_3H_7	i-C_3H_7	8.0 ±2.0	4.0 ± 0.6	26.8 ±1.9
17	n-C_3H_7	c-C_3H_7 [d]	20.7 ±3.5	331 ±37	5.5 ±0.6

#	R^1	R^2			
18	$n\text{-}C_3H_7$	$n\text{-}C_4H_9$	20.9 ±0.9	18.8 ±3.9	26.8 ±1.4
19	$i\text{-}C_3H_7$	$i\text{-}C_3H_7$	4.7 ±1.0	6.5 ±4.0	56.7 ±1.3
20	$i\text{-}C_3H_7$	$c\text{-}C_3H_7$ [d]	25.0 ±4.3	15.8 ± 0.8	14.6 ±0.9
21	$i\text{-}C_3H_7$	$n\text{-}C_4H_9$	14.9 ±0.2	11.6 ±7.3	80.3 ±1.9
22	$c\text{-}C_3H_7$ [d]	$c\text{-}C_3H_7$ [d]	38.6 ±10.5	41.5 ±2.4	42.5 ±2.4
23	$c\text{-}C_3H_7$ [d]	$n\text{-}C_4H_9$	20.8 ±3.6	182 ±9	10.1 ±0.4
24	$n\text{-}C_4H_9$	$n\text{-}C_4H_9$	43.6 ±4.0	50.5 ±0.9	30.4 ±2.1
YM 155			45.9 ±1.0	38.6 ±6.5	ND
Chloroquine			233 ±4	23.4 ±2.6	
Artesunate			13.3(±4.5	22.8 ±2.4	
Atovaquone			2.5 ±1.3	2.8 ±1.2	

[a] To note that R^1/R^2 are interchangeable due to resonance within the imidazolium ring. [b] Concentration corresponding to 50% of the net amount of fluorescence of non-treated control cultures. Mean (± SD) of n = 3 separate determinations. [c] Concentration required to reduce cell growth by 50% relative to untreated cultures as determined by a tetrazolium dye assay. Mean (± SD) of n = 3 separate determinations. [d] $c\text{-}C_3H_7$ = cyclopropyl

To further examine the activity moderating effects of the alkyl residues at R^1/R^2, we prepared Series C which has isobutyl at R^1 and longer alkyl side chains (up to dodecyl) at R^2. These compounds were tested alongside the potent Series A analogs (**11,14,16, 19**) on drug sensitive NF4 and drug resistant K1 and W2 strains using the SYBR Green I fluorescence assay as a proxy of parasite proliferation (Table 2).[16] Interestingly, a total carbon count of 5-6 at R^1/R^2 of Series C was yet again associated with optimal activity. Hence, **25** and **26** which have methyl/ethyl at R^2 have IC_{50} values that were broadly comparable to **11,14,16,19** of Series A. Extending the length of R^2 caused a gradual and uneven decline in activity.

Table 2: $IC_{50}s$ of Series C (**25-35**) and potent Series A analogs (**11,14, 16,19**) on (i) asexual stages of *P. falciparum* NF54 (drug sensitive) and K1,W2 (drug resistant) and (ii) early gametocytes (EG) and late gametocytes (LG) of transgenic parasite line NF54-Pfs16-GFP-Luc.

No	R^{1} [a]	R^{2} [a]	IC_{50} (nM) [b]			Gametocytocidal IC_{50} (nM) [c]	
			NF54	K1	W2	EG	LG
11	C_2H_5	$n\text{-}C_3H_7$	3.45 ±0.31	6.5 ±1.7	4.94 ±0.29	390 ±83	709 ±112
14	C_2H_5	$n\text{-}C_4H_9$	1.64 ±0.2	2.4 ±0.7	2.88 ±0.18	268 ±56	320 ±35
16	$n\text{-}C_3H_7$	$i\text{-}C_3H_7$	2.28 ±0.19	3.1 ±0.8	2.20 ±0.12	162 ±52	567 ±87
19	$i\text{-}C_3H_7$	$i\text{-}C_3H_7$	1.43 ±0.13	2.5 ±1.3	2.18 ±0.16	72 ±5	653 ±29
25	$i\text{-}C_4H_9$	CH_3	1.92 ±0.12	3.40 ±0.40	1.85 ±0.10	41 ±17	1088 ± 26
26	$i\text{-}C_4H_9$	C_2H_5	1.63 ±0.02	3.10 ±0.50	1.62 ±0.14	33 ±5	1019 ±251
27	$i\text{-}C_4H_9$	$n\text{-}C_3H_7$	2.97 ±0.10	4.42 ±0.10	2.12 ±0.16	269 ±48	842 ± 251
28	$i\text{-}C_4H_9$	$i\text{-}C_3H_7$	2.36 ±0.07	4.22 ±0.21	1.96 ±0.30	229 ±79	689 ±138
29	$i\text{-}C_4H_9$	$c\text{-}C_3H_7$	3.94 ±0.23	5.85 ±0.08	2.55 ±0.23	139 ±48	832± 274
30	$i\text{-}C_4H_9$	$n\text{-}C_4H_9$	7.20 ±0.40	9.85 ±0.21	5.10 ±0.50	181 ±87	275 ± 66
31	$i\text{-}C_4H_9$	$i\text{-}C_4H_9$	9.19 ±0.32	12.5 ±0.7	5.75 ±0.27	337 ±65	812 ± 364
32	$i\text{-}C_4H_9$	$n\text{-}C_6H_{13}$	6.20 ±0.15	10.0 ±0.1	5.28 ±0.21	143 ± 9	551 ± 99
33	$i\text{-}C_4H_9$	$n\text{-}C_8H_{17}$	4.36 ±0.08	8.23 ±1.02	3.60 ±0.80	39 ± 18	164 ±10
34	$i\text{-}C_4H_9$	$n\text{-}C_{10}H_{21}$	4.96 ±0.17	13.3 ±2.1	6.10 ±0.40	370 ±73	237 ± 66

35	$i\text{-}C_4H_9$	$n\text{-}C_{12}H_{25}$	4.30 ±0.50	11.2 ±1.0	5.50 ±0.40	361 ±75	174 ± 11
Chloroquine			10 ±3	154 ±14[d]	233 ±40	-	-
Artesunate			3.0 ±0.29	3.26 ±.20	2.40 ±0.20	63 ±3	259 ±80
Methylene Blue			-	-	-	95 ±11	143 ±17

[a] R^1 and R^2 are as depicted in Table 1. [b] Concentration corresponding to 50% of the net amount of SYBR Green I fluorescence of non-treated control cultures. Mean (± SEM) of n = 3 independent biological replicates. [c] Concentration corresponding to 50% reduction of luminescence in early and late gametocytes of NF54-Pfs16-GFP-Luc in a luciferase-based assay. Mean (± SEM) of n = 3 independent biological replicates. [d] IC_{50} of CQ on the *P. falciparum* strain (K1) was 212 (± 32) on the Hoechst assay, indicating broad equivalence between the Hoechst and SYBR Green I assay platforms.

Next, we assessed the compounds in Table 2 for transmission blocking activity on early (>95% stage II/III) and late (> 90% stage IV/V) stage gametocytes.[17] Most compounds were gametocytocidal (IC_{50} < 1000 nM) and generally more potent against early gametocytes (IC_{50} 30-400 nM) than late gametocytes (IC_{50} 160-1100 nM). Indeed, several compounds (**19, 25, 26, 33**) were as cidal as the positive controls artesunate and methylene blue against early gametocytes. There was no discernible trend as to how alkyl chain lengths impacted early gametocytocidal activity in Series C. On the other hand, the potent activity of analogs **33, 35** against late stage gametocytes (comparable to artesunate) alluded to a preference for longer alkyl side chains (total carbon count ≥ 12) at R^1/R^2 against this stage of the life cycle. Noticeably, **33** displayed outstanding potencies against both early and late gametocytes which may suggest its potential in blocking transmission.

The preceding discussion on the effect of R^1/R^2 alkyl chain length on asexual/sexual potencies pointed to a possible moderating role for lipophilicity. To confirm, the clogP values and antimalarial IC_{50}s of Series A and C were analyzed for statistical correlations based on Spearman ρ coefficients (Tables S-3, S-4). Interestingly, no significant correlation between clogP and asexual IC_{50} was detected in Series A but it was observed in Series C (Table S-4). Very likely, the extended clogP range arising from the inclusion of analogs with longer alkyl side chains in Series C led to this outcome. The correlation for Series C was positive (smaller clogP /shorter side chains favored potent activity), recapitulating our preceding anecdotal inferences. When correlations between lipophilicities and gametocytocidal activities (IC_{50} $_{EG}/IC_{50\ LG}$) of Series C were examined, none was observed for early gametocytes but a negative relationship was detected for late gametocytes (longer side chains favored potent activity) (Table S-4).

Thus far, most of the compounds in Table 2 qualified as validated antimalarial hits based on their outstanding potencies against asexual (sensitive and multidrug resistant strains, $IC_{50} <$ 100 nM) and sexual life stages of the parasite.[5] Progression to early lead status would require evidence of *in vivo* efficacy ($ED_{90} < 50$ mg/kg) against the blood stages of infection in a *P. falciparum* infected humanized mouse model.[5] To this end, we selected **19** as a representative member for animal studies. The choice of **19** was primarily motivated by its excellent activity against asexual parasites, exceeding that of the most favored Series C analog **33** which is arguably better positioned in terms of gametocytocidal activity.

Table 3: PK parameters for compound **19** administered to male C57BL6 mice (n=3 per dosing route)

Route	Dose (mg/kg) [a]	t $_{1/2}$ (h)	CL (mL/min/kg)	V_d (L/Kg)	C_{max} (µM)	T_{max} (h)	AUC_{0-last} (min. µmole/L)[b]	% F
Intravenous	2	1.4	70	8.3	-	-	130	-
Oral	20	11.3	-	-	337	2	69	5

Prior to pharmacokinetic (PK) profiling in mice, **19** was assessed for its solubility, PAMPA permeability and liability to metabolic breakdown by rat liver microsomes. **19** had good water solubility (> 100 μM, pH 7.4) but no detectable PAMPA permeability. It was remarkably stable to microsomal degradation (Figure S-1) and additionally, well tolerated in mice when administered intravenously (2 mg/kg) and orally (20 mg/kg). In line with its hydrophilic nature, the PK of **19** revealed limited tissue distribution (volume of distribution Vd 8.3 L/kg), rapid clearance from plasma (CL 70 mL/min/kg) and a relatively short half-life ($t_{1/2}$ 1.4 h) (Table 3). Oral bioavailability was however limited at 5 %, likely due to its quaternized state which would limit permeability across the gastrointestinal barrier. Notwithstanding, a plot of plasma concentration (after oral administration) versus time showed that levels of **19** were well above its $IC_{50\ 3D7}$ for the period of exposure (24 h) (Figure 2).
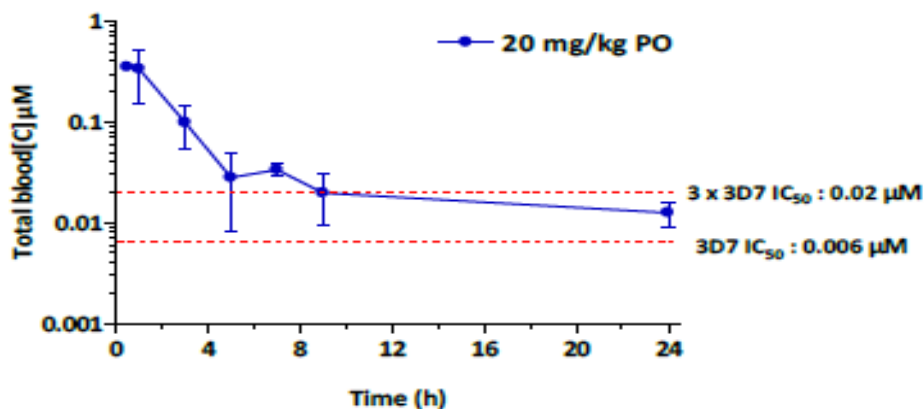
Figure 2: Systemic exposure of **19** over 24 h following administration of a single oral dose (20 mg/kg) to healthy mice over 24 h. Dotted lines embedded within plot are the IC_{50} (1x, 3x) values of **19** against CQ sensitive 3D7 *P. falciparum*.

Thus encouraged, we proceeded to evaluate the efficacy of **19** on a humanized mouse model of *P. falciparum* (*Pf*3D7 [0087/N9]). Briefly, **19** was administered orally at 5 doses ranging from 1 to 50 mg/kg, with each dose given for 4 days (Days 3-6). Parasitemia was determined on each treatment day and on Day 7. The effective dose of **19** required to reduce parasitemia by 90% on Day 7 (ED_{90}) was estimated to be 34 mg/kg (Figure 3). Noting that parasitemia was not reduced significantly at the highest dose, some caution should be accorded to this value.

11

19 could admittedly have greater in vivo efficacy if not for its limited oral bioavailability. Appropriate formulation strategies may be employed to circumvent this liability.
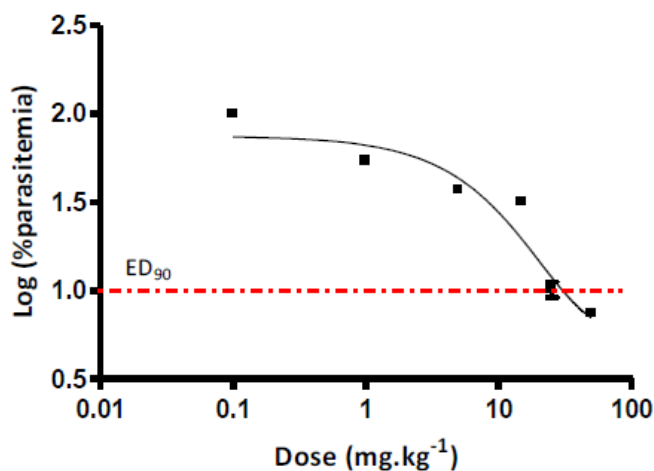

Figure 3: *In vivo* efficacy of **19** on the humanized *P. falciparum* (*Pf*3D7[0067/N9]) mouse model. ED$_{90}$ is the effective dose (mg/kg) required to reduce parasitemia by 90% on Day 7 compared to untreated control animals. It was obtained from non-linear fitting of log parasitemia on Day 7 post-infection versus administered oral dose of **19**. ED$_{90}$ was estimated to be 34 mg/kg.

Taken together, we have identified two features in the scaffold that were consequential to potent antimalarial activity. They are (i) substituents (R^1/R^2) attached to the ring N atoms and (ii) the fused quinone-imidazolium ring. For (i), alkyl side chains at R^1/R^2 are preferred to the ring based residues found in YM155, **1** and **2.** The lipophilicities imparted by the alkyl chains are important drivers of activity but as noted earlier, in disparate ways that were influenced by the phase of the plasmodial life cycle. The requirement (ii) for the fused quinone-imidazolium ring is a puzzle. Quinones are found in several antimalarials and in most instances, they are assumed to disrupt the redox balance in the parasitized erythrocytes through their propensity to redox cycle.[18] Indeed, the potent activity of the antimalarial lead compound plasmadione was attributed to redox cycling by its quinone moiety.[19] In contrast, the low redox potential of the antimalarial drug atovaquone abrogated the role of the quinone in sustaining a subversive substrate-driven redox cycle.[20] Rather, atovaquone acts as competitive inhibitor of the plasmodial cytochrome b quinol oxidation (Qo) site, [21,22] with the quinone providing additional sites of contact to the target through hydrogen bonding.[23] This prompted us to evaluate the potent Series A analogs (**11,14,16,19**) against *P. falciparum* TM90C2B which carries a

mutation in the *cyt b* gene, thus rendering atovaquone inactive against it (Table 4). Interestingly, the compounds were no less active on TM90C2B than on CQ resistant (K1) and sensitive (NF54) strains, thus precluding the mitochondrial cytochrome bc1 complex as a putative target. On the other hand, the same compounds were identified as redox cyclers on the *in vitro* phenol red horse radish peroxidase assay, [24] albeit less effectively than 1,4-naphthoquinone and intriguingly, exceeding that of the non-quaternized Series B compounds which had no detectable redox cycling activity (Table S-5). If these findings are reconfirmed on other assay platforms, it would signal a novel modulating effect by the charged imidazolium on the redox status of the quinone and hence a mechanistic rationale for the structural importance of the quinone-imidazolium entity. Alternatively, noting that YM155 is preferentially taken up by the solute carrier SLC35F2 into malignant cells,[25] it is tempting to accord a facilitatory role to the charged quinone-imidazolium entity with regard to uptake into parasitized erythrocytes.

Table 4: IC_{50} values of Series A analogs (**11,14,16,19**) against *P. falciparum* NF54, K1 and atovaquone-resistant TM90C2B determined by [^{3}H]-hypoxanthine incorporation.

Compound	IC_{50} (nM)			Compound	IC_{50} (nM)		
	NF54 (n=2)	K1 (n=2)	TM90C2B (n=3)		NF54 (n=2)	K1 (n=2)	TM90C2B (n=3)
11	1.2	2.2	2.2	Chloroquine	8.6	144	140
14	1.0	1.8	1.4	Artesunate	3.2	1.4	2.7
16	1.0	2.1	1.8	Atovaquone	0.4	0.5	11500
19	1.0	1.9	1.6				

In conclusion, we have identified the dioxonaphthoimidazolium scaffold as a promising antimalarial pharmacophore, with several members displaying exceptional potencies against sensitive and multidrug resistant asexual parasites (< 100 nM) as well as early and late stage gametocytes (< 1000 nM). The attractiveness of the scaffold from a medicinal chemistry

perspective is further enhanced by its synthetic accessibility, the excellent comparative cytotoxicities of its members, and based on a representative potent analog **19**, good aqueous solubility, metabolic stability and *in vivo* tolerability in mice. The PK profile of **19** revealed limited tissue distribution, rapid plasma clearance and a relatively short half-life. However, **19** had limited oral bioavailability (5%) which arguably contributed to its modest activity in the humanized mouse model of *P. falciparum*. Greater efficacy would conceivably be achieved if not for the poor permeability of **19** arising from its quaternized state. Notwithstanding these PK issues, it is still possible to leverage on the inherent merits of the scaffold by engaging formulation strategies or structural modifications to optimize lipophilicity. Lastly, we have provided clarity on the fundamental structure activity requirements of this class of compounds. Importantly, the quinone is recognized as a necessary but insufficient feature for potent activity. Rather it is the fused quinone-imidazolium entity that is pivotal, plausibly by facilitating cellular entry or fulfilling a mechanistic role in enhancing the reactivity of the quinone. Additionally, lower lipophilicities appear to augment activity against asexual forms whereas higher lipophilicities favoured activity against late stage gametocytes. Future work will focus on addressing the PK limitations of the scaffold through structure modification, establishing a better understanding of the mode of action and exploring interactions of potent members with other antimalarial agents.

ASSOCIATED CONTENT

SUPPORTING INFORMATION

The Supporting Information is available free of charge on the ACS publications website at DOI: xxxx. Description of methods used to synthesize Series A-C compounds; characterization of intermediates and final compounds; purity determination of final compounds; synthesis of target compound **19**, NMR and HPLC Spectra of **19**; activity of Series B on asexual stages of NF54 *P. falciparum;* cLogP values of Series A and C; Spearman ρ correlation coefficients of Series A and C; solubility, PAMPA permeability and microsomal stability of **19;** redox cycling EC$_{50}$ values of Series A and B as determined by the phenol red horse radish peroxidase assay; cytotoxicities of Series A compounds on Chinese Hamster Ovary (CHO) cells; in vitro assessment of antimalarial activity against asexual forms and gametocytes of *P. falciparum* **;** pharmacokinetic analysis of **19** in mice; in vivo efficacy of **19** in a humanized mouse model of *P. falciparum*;

AUTHOR INFORMATION

Corresponding Authors

* Mei-Lin Go; Email phagoml@nus.edu.sg; Tel: +65-65162654.

Richard K. Haynes; Email richard.haynes@nwu.ac.za; Tel: +27(0)182994466.

AUTHOR CONTRIBUTIONS

The manuscript was written through contributions of all authors. ‡ These authors (SA, DC, JXT) contributed equally.

NOTES

The authors declare no conflicting financial interests.

REFERENCES

(1) World Health Organization, *World Malaria Report 2018*, Geneva, 2018.

(2) Burrow, J.N.; Duparc, S.; Gutteridge, W.E.; van Huijsduijnen, R.H.; Kaszubska, W.; Macintyre, F.; Mazzuri, S.; Mohrle, J.J.; Wells, T.N.C. New developments in anti-malarial target candidate and product profiles. *Malar. J.* **2017,** *16,* 26.

(3) Hamilton, W.L.; Armato, R.; van der Pluijm, R.W.; Jacob, C.G.; Quang, H.H.; Thuy-Nhien, N.T.; Hien, T.T.; Hongvanthong, B.; Chindavongsa, K.; Mayxay, M.; Huy, R.; Leang, R.; Huch, C.; Dysoley, L.; Amaratunga, C.; Suon, S.; Fairhurst, R.M.; Tripura, R.; Peto, T.J.; Sovann, Y.; Jittamala, P.; Hanboonkunupakarn, B.; Pukrittayakamee, S.; Chau, N.J.; Imwong, M.; Dhorda,

M.; Vongpromek, R.; Chan, X.H.S.; Maude, R.J.; Pearson, R.D.; Nguyen, T.; Rockett, K.; Drury, E.; Goncalves, S.; White, N.J.; Day, N.P.; Kwiatkowski, D.P.; Dondorp, A.M.; Miotto, O. Evolution and expansion of multi-drug resistant malaria in Southeast Asia: a genomic epidemiology study. *Lancet Infect. Dis.* **2019,** published online July 22 2019; DOI: 10.1016/S1473-3099(19)30392-5.

(4) Owen, S. Malaria and the millennium development goals. *Arch. Dis. Child.* **2015,** *100,* 53-56.

(5) Katsuno, K.; Burrows, J. N.; Duncan, K.; Hooft, V. H. R.; Kaneko, T.; Kita, K.; Mowbray, C. E.; Schmatz, D.; Warner, P.; Slingsby, B. T. Hit and lead criteria in drug discovery for infectious diseases of the developing world. *Nat. Rev. Drug Discov.* **2015**, *14*, 751-758.

(6) Tanaka, T.Q.; Guiguemde, W.A.; Barnett, D.S.; Maron, M.I.; Connelly, M.C.; Suryadevara, P.K.; Guy, R.K.; Williamson, K.C. Potent Plasmodium falciparum gametocytocidal activity of diaminonaphthoquinones, lead antimalarial chemotypes identified in an antimalarial compound screen. *Antimicrob. Agents Chemother.* **2015,** *59,* 1389-1397.

(7) Ho, S.H.; Sim, M.Y.; Yee, W.L.; Yang, T.; Yuen, S.P.; Go, M.L. Antiproliferative, DNA intercalation and redox cycling activities of dioxonaphtho[2,3-d]imidazolium analogs of YM155: A structure-activity relationship study. *Eur. J. Med. Chem.* **2015,** *104,* 42-56.

(8) Yamanaka, K.; Nakata, M.; Kaneko, N.; Fushiki, H.; Kita, A.; Nakahara, T.; Koutoku, H.; Sasamata, M. YM155, a selective surviving suppressant, inhibits tumor suppressant, inhibits tumor spread and prolongs survivial in a spontaneous metastatic model of human triple negative breast cancer. *Int. J. Oncol.* **2011,** *39,* 569-575.

(9) Kuznetsov, V.S.; Efros, L.S. Heterocyclic derivatives of substituted 1,4-naphthoquinones. VI. Derivatives of naphtho[2,3-d]imidazole-4,9-dione. *Zh. Org. Khim.* **1967,** *3*, 393-402.

(10) Truitt, P.; Hayes, D; Creagh, L.T. 1,2-Disubstituted naphtha[2,3-d]imidazole-4,9-diones and corresponding quaternary salts. *J. Med. Chem.* **1964,** *7,* 362-364.

(11) Wei, Q.; Li, J.; Tang, F.; Yun, Y.; Zhao, Y.; Yao, Q. Synthesis and biological evaluation of novel 2-arylvinyl-substituted naphtha[2,3-d]imidazolium halide derivatives as potent antitumor agents. *Eur. J. Med. Chem.* **2018,** *144,* 504-516.

(12) Inagaki, Y. Preparation of naphthimidazolium salts as dye intermediates. *Jpn. Kokai Tokkyo Koho*, **1991,** JP 03258765 A 19911119.

(13) Yan, D.; Zhang, W.; Zhang, Z.; Liu, Z. Process for preparation of 1,4-naphthoquinone/anthraquinone imidazole derivative for treating tumor. **2018**, CN 108530365.

(14) Tong, J.X.; Chandramohanadas, R.; Tan, K.S.W. High-content screening of the Medicines for Malaria Venture Pathogen Box for Plasmodium falciparum digestive vacuole disrupting molecules reveals valuable starting points for drug discovery. *Antimicrob. Agents Chemother.* **2018,** *62,* e02031-17.

(15) Talele, T.T. The "cyclopropyl fragment" is a versatile player that frequently appears in preclinical/clinical drug molecules. *J. Med. Chem.* **2016,** *59,* 8712-8756.

(16) Johnson, J.D.; Dennull, R.A.; Gerena, L.; Lopez-Sanchez, M.; Roncal, N.E.; Waters, N.C. Assessment and continued validation of the malaria SYBR green I-based fluorescence assay for use in malaria drug screening. *Antimicrob. Agents Chemother.* **2007,** *51,* 1926-1933.

(17) Reader, J.; Botha, M.; Theron, A.; Lauterbach, S.J.; Rossouw, C.; Engelbrecht, D.; Wepener, M.; Smit, A.; Leroy, D.; Mancama, D.; Coetzer, T.L.; Birkholtz, L.M. Nowhere to hide: Interrogating different metabolic parameters of Plasmodium falciparum gametocytes in a transmission blocking drug discovery pipeline towards malaria elimination. *Malar. J.* **2015,** *14,* 213.

(18) Sidorov, P.; Desta, I.; Chesse, M.; Horvath, D.; Marcou, G.; Varnek, A.; Davioud-Charvet, E.; Elhabiri, M. Redox polypharmacology as an emerging strategy to combat malaria parasites. *ChemMedChem.* **2016,** *11,* 1-14.

(19) Ehrhardt, K.; Deregnaucourt, C.; Goetz, A.; Tzanova, T.; Gallo, V.; Arese, P.; Pradines, B.; Adjalley, S.H.; Bagrel, D.; Blandin, S.; Lanzer, M.; Davioud-Charvet, E. The redox cycler plasmodione is a fast-acting antimalarial lead compound with pronounced activity against sexual and early asexual blood-stage parasites. *Antimicrob. Agents Chemother.* **2016,** *60,* 5146-5158.

(20) Ehrhardt, K.; Davioud-Charvet, E.; Ke, H.; Vaidya, A.B.; Lanzer, M.; Deponte, M. The antimalarial activities of methylene blue and the 1,4-naphthoquinone 3-[4-(trifluoromethyl)benzyl]-menadione are not due to inhibition of the mitochondrial electron transport chain. *Antimicrob. Agents Chemother.* **2013,** *57,* 2114- 2120.

(21) Fry, M.; Pudney, M. Site of action of the antimalarial hydroxynaphthoquinone, 2-[trans-4-(4'-chlorophenyl) cyclohexyl]-3-hydroxy-1,4-naphthoquinone (566C80). *Biochem. Pharmacol.* **1992,** *43,* 1545-1553.

(22) Srivastava, I.K.; Rottenberg, H.; Vaidya, A.B. Atovaquone, a broad spectrum antiparasitic drug, collapses mitochondrial membrane potential in a malarial parasite. *J. Biol. Chem.* **1997,** *272,* 3961-3966.

(23) Nixon, G.L.; Moss, D.M.; Shone, A.E.; Lalloo, D.G.; Fisher, N.; O'Neill, P.M.; Ward, S.A.; Biagini, G.A. Antimalarial pharmacology and therapeutics of atovaquone. *J. Antimicrob. Chemother.* **2013,** *68,* 977-985.

(24) Johnson, P.A.; Soares, K.M.; Shinde, S.N.; Foster, C.A.; Shun, T.Y.; Takyi, H.K.; Wipf, P.; Lazo, J.S. Development of a 384-well colorimetric assay to quantify hydrogen peroxide generated by the redox cycling of compounds in the presence of reducing agents. *Assay Drug Dev. Technol.* **2008,** *6,* 505-518.

(25) Winter, G. E.; Radic, B.; Mayor-Ruiz, C.; Blomen, V. A.; Trefzer, C.; Kandasamy, R. K.; Huber, K. V. M.; Gridling, M.; Chen, D.; Klampfl, T.; Kralovics, R.; Kubicek, S.; Fernandez-Capetillo, O.; Brummelkamp, T. R.; Superti-Furga, G. The solute carrier SLC35F2 enables YM155-mediated DNA damage toxicity. *Nat. Chem. Biol.* **2014,** *10,* 768-773.

Table of Contents Graphic

Pf Asexual IC$_{50}$ nM
NF54 1.4   K1 2.4
W2 2.2 TM90C2B 1.6

Pf Gametocytes IC$_{50}$ nM
NF54-Pfs 16-GFP-Luc
Early stage   70
Late stage   650

Pf efficacy *in vivo* humanized mouse model 34 mg/kg